This article has been accepted for publication in a future issue of this journal, but has not been fully edited. Content may change prior to final publication. Citation information: DOI 10.1109/LPT.2014.2310638, IEEE Photonics Technology Letters

Experimental Demonstration of 50 Mb/s Visible Light Communications using 4×4 MIMO

Andrew Burton, Hoa Le Minh, Zabih Ghassemlooy, Edward Bentley and Carmen Botella

***Abstract*— This letter reports the experimental demonstration of an indoor visible light non-imaging multiple input multiple output (MIMO) system with an aggregate error free bit rate of 50 Mb/s over a distance of 2 m. The system uses four independent white LED transmitters, each transmitting 12.5 Mb/s of data in the on-off keying non-return zero (OOK-NRZ) format, and four independent non-imaging optical receivers. The performance of four detection methods ranging from the basic channel inversion to the more advanced space time techniques is compared experimentally. The results gathered demonstrate that the simplest technique is capable of the same bit error rate (BER) as the most complex scheme. The system also provides full illumination with a mean level of 350 Lux satisfying the ISO lighting standards for home and office environments.**

***Index Terms*— VLC, MIMO, non-imaging, ZF, Pseudo inverse, MMSE, V-BLAST**

I. Introduction

Visible light communications (VLC) MIMO is becoming popular due to its ability to increase the transmission data rate. In a mobile environment, simultaneously transmitting parallel data streams through the use of several lighting units typically employed to provide uniform room illumination allows increased data throughput. In [1] a 1 Gb/s 4 × 9 VLC-MIMO link (1 m range with a small optical footprint) is demonstrated using an imaging lens, and where pre and post equalization have been employed to extend the system bandwidth. The orthogonal frequency division multiplexing (OFDM) modulation format was implemented with adaptive bit and power-loading, requiring a feedback link. So far in VLCs there is no unanimous agreement on a suitable uplink.

In [2], an artificial neural network based VLC-MIMO non-imaging system with a data rate of 1.8 Mb/s was demonstrated. The link length in this study was 10 cm (around 20 times less than in this work) and was based on an organic photodetector with a dynamic ~ 130 – 180 kHz bandwidth.

A spatial VLC-MIMO technique is described in [3] where just a single transmitter (Tx) is active at any time. While this configuration avoids interference between different transmitters, it does not allow a significantly improved data rate due to the lack of parallel transmission and is therefore not an optimal solution for future VLC-MIMO systems.

Finally, in [4] simulations of a 4 × 4 non-imaging VLC MIMO were proposed. The number of LEDs in each Tx unit was set to 3,600, which seems an unrealistic number for commercial deployment. Furthermore, in [4] the blind spots on the receiving plain (RP) were found where decomposition of the transmitted signals cannot occur due to the symmetry in the system geometry. In this letter, we show that in a practical system a perfect symmetry is difficult to achieve, removing the need for an imaging lens, which in turn reduces the overall cost and complexity of the system.

MIMO systems have been studied extensively for radio frequency (RF) applications [5, 6] and are now being adopted in optical communications. The work reported in this letter presents the first practical demonstration of a long range (2 m) non-imaging VLC MIMO system. Four methods of data recovery are tested with increasing levels of complexity to de-multiplex the received data; these are zero forcing (ZF), ZF with pseudo inversion, minimum mean square error (MMSE) and vertical Bell labs layered space time (V-BLAST) algorithms. With the use of a single RC post equalization stage (as in [7]) and the de-multiplexing techniques, error free 50 Mb/s transmissions can be achieved with OOK NRZ at a distance of 2 m whilst simultaneously providing full ISO standard illumination. In comparison to the 4 MHz system this shows an increase in data rate of 12.5 times, which to the best of our knowledge is the fastest presently recorded for the non-imaging VLC MIMO systems for home/office lighting environments.

II. VLC Non-Imaging Multiple Input Multiple Output Channel Model And Detection Methods

A schematic for the non-imaging VLC MIMO system is shown in Fig. 1. The input data $\boldsymbol{X}$ is multiplexed into t-parallel transmit data streams x_j (j = 1,...,t). Each of the new data streams are used to intensity modulate a light source, Tx_j (j = 1,...,t). As all data streams are transmitted at the same time, the received signal is a linear combination of all x_j. In order to de-multiplex the signals and retrieve the transmitted data, the MIMO system has first to estimate the channel coefficients between a pair of Tx and receiver (Rx). To achieve this, pilot signals are periodically inserted into the data so as when one pilot signal is active the remaining transmitters are silent;

Manuscript received November 20, 2013. This work was supported by Northumbria University and by the EU COST ACTION IC1101.

A. Burton, H. Le Minh, Z. Ghassemlooy and E. Bentley are with the Faculty of Engineering and Environment, Optical Communications Research Group, Northumbria University, Newcastle-upon-Tyne NE1 8ST, U.K. (email andrew.burton{ hoa.le-minh, z.ghassemlooy, Edward.bentley} @northumbria.ac.uk).

C. Botella is with the Group of Information and Communication Systems (GSIC), Institute of Robotics and Information & Communication Technologies (IRTIC), University of Valencia, 46980, Valencia, Spain (email Carmen.Botella@uv.es)

This article has been accepted for publication in a future issue of this journal, but has not been fully edited. Content may change prior to final publication. Citation information: DOI 10.1109/LPT.2014.2310638, IEEE Photonics Technology Letters

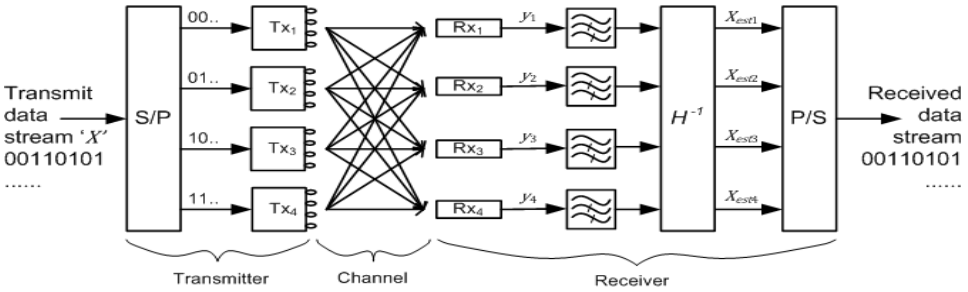

Fig. 1 4×4 VLC Non-imaging MIMO block diagram

hence each pilot is transmitted during a unique time slot as in [2, 7]. On receiving all pilot signals, a **H** matrix detailing the received optical powers is logged. It is only then that the Tx's can proceed with the simultaneous transmission of data on all channels. The received signals can be expressed by:

$$+\boldsymbol{n}. \tag{1}$$

The elements in (1) can be further expanded into:

(2)

with $\boldsymbol{y_r}$ is the signal at the r^{th} Rx and $\boldsymbol{n_r}$ a vector denoting the additive white Gaussian noise. The elements h_{tr} are the line of sight (LOS). As LED based transmitters are Lambertian, the luminous intensity in angle $\emptyset$ is given by [8]:

(3)

where I is the total luminous flux of the LED, m is the order of Lambertion radiation determined by the semi-angle for half illuminance of an LED ($\emptyset_{1/2}$ as $m = -\ln 2/\ln(\cos\emptyset_{1/2})$) and $\emptyset$ is the angle of irradiance. Thus the LOS DC channel gain h_{tr} between the t^{th} Tx and r^{th} Rx is given by [8]:

(4)

where A_{det} represents the active area of PD, d_{tr} is the distance between the LED and the detector, ψ is the angle of incidence and $g(\psi)$ is the gain of the optical concentrator given by [8]:

(5)

where n_i denotes the refractive index and Ψ_c denotes the angular field of view (FOV). The simplest method to estimate the transmitted data would be to invert **H** and multiply it with the received vector $\boldsymbol{y}$ known as the ZF:

(6)

where **W** is the beamformer $\mathbf{H^{-1}}$. However, as can be seen from (6), if the values of **H** are low, the noise vector $\boldsymbol{n}$ increases leading to noise amplification [9]. If **H** is rank deficient, then matrix inversion cannot be performed. In such cases, the pseudo inverse of **H** can be used given by [10]:

(7)

where $\mathbf{H}^{\ddagger H}$ is the conjugated transpose of **H**. An estimate of $\boldsymbol{x}$ can then be made by substituting (7) into (6); however, as before, this will also result in noise amplification. A regularized inversion of **H** can be performed using the MMSE detection method. This is designed to minimize the error between the received and transmit vectors [10], and is resilient towards noise enhancement. The pseudo inverse **G** of **H** is chosen so that:

$$\}\}, \tag{8}$$

where $E\{.\}$ denotes expectation, $\mathbf{G}\boldsymbol{y}$ is the estimate of the transmitted vector, and $\boldsymbol{x}$ is the transmitted vector. The matrix **G** can therefore be shown to be [11]:

(9)

where σ_n^2 is the Rx noise power variance, $\mathbf{I}_N$ is a $[t \times t]$ identity matrix and ρ is the average transmission power. An estimate of $\boldsymbol{x}$ can then be recovered, as in (6) replacing **W** with **G** before processing.

The non-linear detection method V-BLAST employs ordered successive interference cancelation, as the impact of each estimated symbol is canceled from the received signal vector $\boldsymbol{y}$ [11, 12]. It is a computationally intense iterative process whereby the inverse of **H** ((6) to (9) for example), is taken to estimate symbols from the strongest signal, before canceling that symbol from$\boldsymbol{y}$. This effectively reduces the size of **H** from $r \times t$ to $r \times [t-1]$. The inverse of the new **H** is then used to estimate the next symbol, after which the process is repeated until the last symbol has been found. The advantage for using this method is the increase in diversity as the iteration process progresses; however, any errors will propagate with each iteration. Other methods for decoding $\boldsymbol{y}$ exists such as the singular value decomposition [13] involving pre-coding of the transmitted data. This requires channel state information (CSI) at Tx, which is not trivial and usually requires a feedback link, hence is not considered for this application. Other standard MIMO techniques such as the sphere decoding with maximum likelihood detector [14] as well as the lattice-reduction-aided detection [15] are available but are also not considered here.

III. Experimental Setup

A. System description

An experimental system is devised to demonstrate and evaluate the proposed MIMO system with four different detection schemes. The system setup based on Fig.1 consists of four independent Tx's (Fig. 2(a)), and four independent Rx's (Fig. 2(b)). Each Tx is composed of an array of four high power Luxeon Rebel white phosphor LEDs acting as a single source, i.e. they all carry the same signal. Each Rx consists of a concentration lens, a PIN photodiode and a transimpedance amplifier (AD8015) that feeds into a post amplifier prior to RC equalization. Transmitters are fed with the cyclic and independent OOK NRZ pseudo random data of length 2^{10}-1 at 12.5 Mb/s. The received signals are recorded on a real time

This article has been accepted for publication in a future issue of this journal, but has not been fully edited. Content may change prior to final publication. Citation information: DOI 10.1109/LPT.2014.2310638, IEEE Photonics Technology Letters

oscilloscope (DSO9254A) and are processed offline. All system parameters are given in Table I.

Table I System parameters

Parameter	Value
4 × LED Transmitters	
Bit rate per channel R_B	12.5 Mb/s
LED pitch	5 cm
Transmitter pitch	25 cm
Optical transmitter power (per LED)	175 mW
Modulation depth	0.45
Modulation bandwidth	4 MHz
Beam angle (full)	120°
Channel	
Test area $w \times l \times h$	1.4×1.7×2 m^3
4 × Optical Receivers	
PD (OSD15-5T) reverse bias	50 VDC
Lens *diameter/ focal length*	25 mm / 25 mm
Receiver field of view (FOV) (full)	30°
Receiver pitch	20 cm
LPF cut-off frequency	0.75* R_B MHz

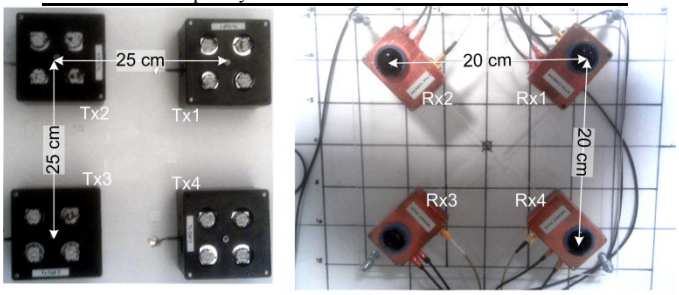

Figure 2 (a) 2×2 transmitter array, and (b) 2×2 receiver array

In this study we only consider the LOS component of the signal, as a root mean square delay spread investigation of the test area has shown that no multipath interference will occur at data rates below 230 Mb/s [16].

B. Experimental procedure

The four receivers are uniformly spread 20 cm apart (as to ensure adequate spatial diversity for **H** matrix not to be singular); with the central position denoting the overall location of the receiving array relative to the receiving plane. A grid set up for measurement, 2 m below the transmitters, was divided into 5×5 cm^2 squares. The centre point of the grid is aligned directly over the centre of the four transmitters (with Cartesian coordinates of [0, 0]).

IV. Experimental Results and Discussion

To begin with, illuminance levels were measured and are shown in Fig. 3. Fig. 3(a) demonstrates that the lighting footprint is approximately 1 m^2 for satisfying the minimum ISO requirement of 300 Lux for illumination. Fig. 3(b) shows the illuminance in the centre of the room at different distances from the transmitters.

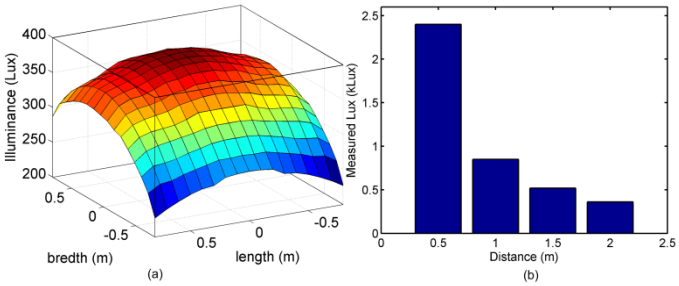

Fig. 3 Measured illuminance: (a) throughout the RP, and (b) centre of the RP at different distances from the Tx's.

The results displayed in Fig. 4 show the collective BER from all four channels MIMO system. Fig. 4 (a) demonstrates the error free operation (BER of 10^{-6}) within a coverage area of 400 cm^2 (20×20 cm^2) using the ZF algorithm. Figs. 4(b)-(d) depict a comparison between the four receivers along the middle row (b), top row (c) and far right hand column (d). In all cases it is shown that there is little or no difference between the four methods. For the Pseudo inverse Rx, when the inverse of **H** exists (7) simply reduces to ZF. It can also be seen from MMSE Rx that with a high SNR (9) will also reduce to ZF. However, when SNR is low we do see a minor improvement in BER (Figs. 4(c-d)). V-BLAST algorithm also shows no improvement over ZF even though it is the most complex and requiring more computation time. The strong similarity between receivers, even for the worst conditioned **H**, is because MIMO strongly relies on non-LOS and LOS CSI, however for this application we only consider the LOS CSI.

Fig. 5 illustrates that channel errors have strong correlation with the spatial positioning of the Rx array in relation with the associated Tx. Hence the errors from channel 1 only appear along the column that happens to be the greatest distance between Tx1 (top right hand corner) and the receivers (positioned to the far left) where the SNR of the particular channel is at its lowest level. Likewise, errors from channels 2-4 occur under similar conditions.

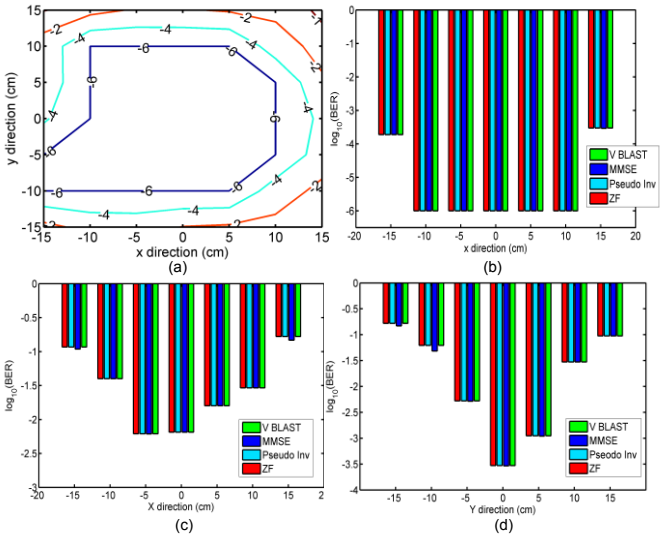

Fig. 4 - overall system BER: (a) in log10(BER) scale using ZF algorithm, (b) BER along middle row in *x* direction, (c) BER along the top row in the *x* direction, and (d) the BER down the far right column in the *y* direction.

Q-factor analysis of the signal between a single Tx and single Rx as a function of the horizontal displacement beneath the centre point of a Tx has been carried out to show at what distance and how fast the quality of the signal degrades. Fig. 6(a) shows the measured *Q*-factor for the channel, using 12 Mb/s OOK NRZ. For OOK NRZ we have the following relationship $BER = 0.5 * erfc(\mathrm{Q}/\sqrt{2})$, where *erfc*(.) is the complementary error function; hence the predicted BER at 15, 20 and 25 cm are 1e-8, 4.4e-5 and 1.6e-2, respectively. Extrapolating this data to estimate the performance of a single input single output (SISO) link, the $\log_{10}$(BER) performance is shown in Fig. 6(b).

Each of the four transmitters are situated 12.5 cm away from the centre of the grid in both *x* and *y* directions. Fig. 6(b)

This article has been accepted for publication in a future issue of this journal, but has not been fully edited. Content may change prior to final publication. Citation information: DOI 10.1109/LPT.2014.2310638, IEEE Photonics Technology Letters

depicts a single Tx with the BER displayed at radius of 15, 20 and 25 cm. Comparing Figs. 4 and 6(b) we notice that employing MIMO has significantly improved the BER performance and the coverage span of each Tx-Rx pair over the SISO system (it must be noted here that for Fig. 4 $\log_{10}(BER) < -6$ has been set to -6). Comparing Figs. 3 and 4 we observe that the proposed MIMO functions only in the centre of the illuminated area, defined by the Tx and Rx separation. Moving the receivers closer to the transmitters would improve the SNR however, due to the limited FOV would see less of the transmitters hence leading to a reduced communications coverage area. Likewise, moving the receivers further away from the transmitters would result in reduced SNR but increased coverage the area over which the receivers can view. As the proposed MIMO system is dependent upon the SNR, the communications area would also decrease.

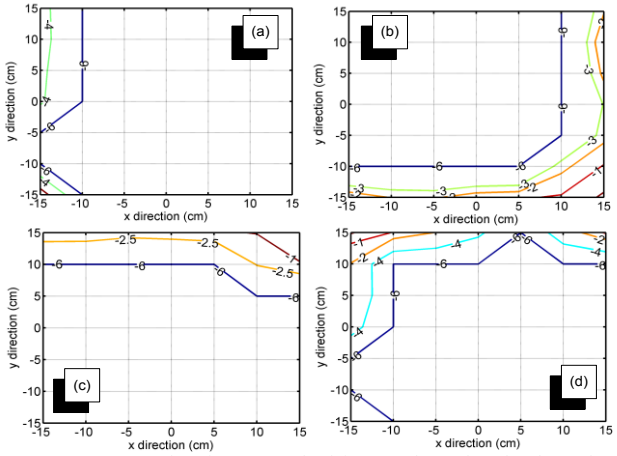

Fig. 5 Log_{10}(BER) totals using ZF method for: (a) channel 1, (b) channel 2, (c) channel 3, and (d) channel 4. The measured $\log_{10}$(BER) are indicated along the isolines.

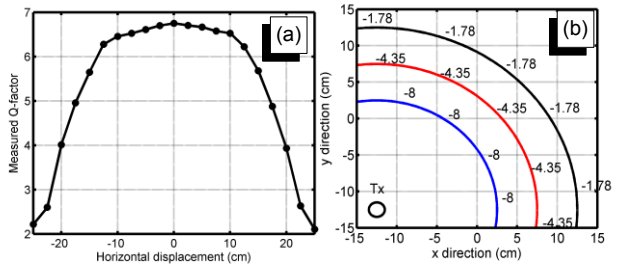

Fig. 6 (a) *Q*-factor with horizontal displacement; (b) estimated BER for SISO link The $\log_{10}$(BER) are indicated along the isolines

V. Conclusion And Future Work

This paper has described a non-imaging 4×4 VLC MIMO system operating error free at 50 Mb/s over a distance of 2 m whilst providing a mean illumination level of 350 Lux. Four de-multiplexing techniques were used for the same data rate, with results showing that the ZF Rx with the least complexity displayed similar behavior and performance compared to higher complexity methods tested under the setup conditions. The operating coverage area of 400 cm^2 was bound by the FOV of the receivers. The experiments have also shown that each pair of Tx and Rx in the MIMO system outperforms SISO. The predominant factor governing the system performance has been found to be the SNR of each channel at the Rx related to the FOV of the Rx array. With a lens at the Rx, the received signal fades fast once the FOV has been surpassed. In order to increase the communications footprint, link adaption based on CSI feedback to the transmitters should be considered, as this is common place for MIMO radio links [17-19]. Employing both pre and post processing the channel is corrupted only by Gaussian noise in front of the detectors [18]. Hence when the channel matrices are singular and poor rank, in this case due the geometrical effects; power, rate adaption and coding can be used to improve system performance.

References

[1] A. H. Azhar, T. A. Tran, and D. O'Brien, "A Gigabit/s indoor wireless transmission using MIMO-OFDM visible-light communications," *Photonics Technology Letters, IEEE,* vol. 25, pp. 171-174, 2013.

[2] P. A. Haigh, Z. Ghassemlooy, I. Papakonstantinou, F. Arca, S. F. Tedde, O. Hayden, and S. Rajbhandari, "A MIMO-ANN system for increasing data rates in organic visible light communications systems," IEEE ICC 2013 , Budapest, Hungary, 2013.

[3] R. Mesleh, R. Mehmood, H. Elgala, and H. Haas, "Indoor MIMO optical wireless communication using spatial modulation," *ICC,* pp. 1-5, 2010.

[4] L. Zeng, D. O'Brien, H. L. Minh, G. Faulkner, L. Kyungwoo, J. Daekwang, O. YunJe, and W. Eun Tae, "High data rate multiple input multiple output (MIMO) optical wireless communications using white led lighting," *Selected Areas in Communications, IEEE Journal on,* vol. 27, pp. 1654-1662, 2009.

[5] T. Haustein and U. Kruger, "Smart geometrical antenna design exploiting the LOS component to enhance a MIMO system based on rayleigh-fading in indoor scenarios," *PIMRC 2003. 14th IEEE Proceedings on*, pp. 1144-1148, 2003.

[6] P. F. Driessen and G. J. Foschini, "On the capacity formula for multiple input-multiple output wireless channels: A geometric interpretation,". *ICC'99 IEEE*, pp. 1603-1607. *1999*

[7] H. L. Minh, D. O'Brien, G. Faulkner, L. Zeng, L. Kyungwoo, J. Daekwang, O. YunJe, and W. Eun Tae, "100-Mb/s NRZ visible light communications using a postequalized white LED," *Photonics Technology Letters, IEEE,* vol. 21, pp. 1063-1065, 2009.

[8] T. Komine and M. Nakagawa, "Fundamental analysis for visible-light communication system using LED lights," *Consumer Electronics, IEEE Transactions on,* vol. 50, pp. 100-107, 2004.

[9] S. Pingping, K. Sooyoung, and C. Kwonhue, "Soft ZF MIMO detection for turbo codes," *WiMob*, pp. 116-120*,* 2010.

[10] C. Peel, Q. Spencer, A. L. Swindlehurst, and B. Hochwald, "Downlink transmit beamforming in multi-user MIMO systems," in *Sensor Array and Multichannel Signal Processing Workshop Procs.*, pp. 43-51*, 2004.*

[11] S. N. Sur, D. Ghosh, D. Bhaskar, and R. Bera, "Contemporary MMSE and ZF receiver for V-BLAST MIMO system in Nakagami-m fading channel," *INDICON*, pp. 1-5, 2011.

[12] P. W. Wolniansky, G. J. Foschini, G. D. Golden, and R. Valenzuela, "V-BLAST: an architecture for realizing very high data rates over the rich-scattering wireless channel,". *ISSSE*, pp. 295-300, 1998

[13] G. Lebrun, S. Spiteri, and M. Faulkner, "Channel estimation for an SVD-MIMO System," in *Communications, IEEE International Conference on*, pp. 3025-3029 Vol.5, 2004

[14] G. Zhan and P. Nilsson, "Algorithm and implementation of the K-best sphere decoding for MIMO detection," *Selected Areas in Communications, IEEE Journal on,* vol. 24, pp. 491-503, 2006.

[15] Y. Huan and G. W. Wornell, "Lattice-reduction-aided detectors for MIMO communication systems," *GLOBECOM,. IEEE*, vol.1., pp. 424-428 , 2002

[16] Z. Ghassemlooy, W. Popoola, and S. Rajbhandari, *Optical Wireless Communications: System and Channel Modelling*: CRC PressINC, 2012.

[17] C. Seong Taek, A. Lozano, and H. C. Huang, "Approaching eigenmode BLAST channel capacity using V-BLAST with rate and power feedback," in *Vehicular Technology Conference, 2001. VTC 2001 Fall. IEEE VTS 54th*, 2001, pp. 915-919 vol.2.

[18] V. Jungnickel, T. Haustein, V. Pohl, and C. Von Helmolt, "Link adaptation in a multi-antenna system," in *VTC 2003-Spring. The 57th IEEE Semiannual*, 2003, pp. 862-866 vol.2.

[19] M. Schellmann, V. Jungnickel, A. Sezgin, and E. Costa, "Rate-Maximized Switching Between Spatial Transmission Modes," in *ACSSC '06. Fortieth Asilomar Conference on*, 2006, pp. 1635-1639.